DOI:
10.1002/anie.202200064

Document Version
Peer reviewed version

Super-robust Xanthine-Sodium Complexes on Au(111)

Chong Chen,[†,§] Pengcheng Ding,[†,‡,||] Zhuo Li,[†,||] Guoqiang Shi,[†] Ye Sun,[‡] Lev N. Kantorovich,[⊥] Flemming Besenbacher,[#,] and Miao Yu[†,||*]*

[†]School of Chemistry and Chemical Engineering, Harbin Institute of Technology, Harbin 150001, China

[‡]School of Instrumentation Science and Engineering, Harbin Institute of Technology, Harbin 150001, China

[§]School of Chemistry and Chemical Engineering, Suzhou University, Suzhou 234000, China

[||]State Key Laboratory of Molecular Reaction Dynamics, Dalian Institute of Chemical Physics, Chinese Academy of Sciences, Dalian 116023, China

[⊥]Department of Physics, King's College London, The Strand, London WC2R 2LS, United Kingdom

[#]iNANO and Department of Physics and Astronomy, Aarhus University, Aarhus 8000, Denmark

* Corresponding author.

Correspondence to: miaoyu_che@hit.edu.cn and fbe@inano.au.dk

ABSTRACT: A widely-accepted theory is that life originated from the hydrothermal environment in the primordial ocean. Nevertheless, the low desorption temperature from inorganic substrates and the fragileness of hydrogen-bonded nucleobases do not support the required thermal stability in such an environment. Herein, we report the super-robust complexes of xanthine, one of the precursors for the primitive nucleic acids, with Na. We demonstrate that the well-defined xanthine-Na complexes can only form when the temperature is $\geq$ 430 K, and the complexes keep adsorbed even at ~720 K, presenting as the most thermally stable organic polymer ever reported on Au(111). This work not only justifies the necessity of high-temperature, Na-rich environment for the prebiotic biosynthesis but also reveals the robustness of the xanthine-Na complexes upon the harsh environment. Moreover, the complexes can induce significant electron transfer with the metal as inert as Au and hence lift the Au atoms up.

INTRODUCTION

Being the most decisive process in the origin of life, the evolution from individual biomolecules to functional oligomers/polymers, and hence to primitive forms of life, remains particularly intriguing yet mysterious over centuries.[1–2] A widely accepted theory is that life originated from the hydrothermal environment [550–670 K][3] that induced by volcano eruption in the primordial ocean.[4–5] Nevertheless, the accumulation hence polymerization of biomolecules on inorganic substrates is regarded to be crucial for the evolution of biomolecular systems,[6–8] whereas the reported desorption temperatures of the DNA bases are far less than 550 K.[9–10] Moreover, although molecular recognition based on hydrogen bonding (the most primary interaction between nucleobases) can already occur at room temperature,[11,12] such bonding can easily be broken even at 483 K.[13] How could the high-temperature submarine environment be appropriate and indispensable for the synthesis of initial form(s) of life then?

Although it is highly difficult to restore the actual picture of primordial submarine synthesis, shedding light on this puzzle through simplified cases is feasible. In this work, we investigate the complexes of xanthine (3,7-dihydro-purine-2,6-dione, $C_5H_4N_4O_2$, Scheme 1) and sodium (Na) on the Au(111) surface. Xanthine is a typical purine base, prevailingly distributed not only in human tissues and fluids,[14,15] but also in prokaryote and eukaryote cells--the earliest life forms on the earth.[16] This compound was present in the ancient solar system and found in high concentrations in extraterrestrial meteorites.[17] Moreover, xanthine has been demonstrated as one of the original exogenous nucleobases abundant on the prebiotic Earth,[18] serving as one of the precursors for the primitive nucleic acids.[19] Na is a vital element in animals and plants.[20] Concentration of Na ions in the primitive ocean was proposed to be 1.5–2.0 folds as that in the modern ocean.[21] It has been suggested that the

presence of Na is capable to accelerate the self-assembly of nucleobases at the liquid-solid interfaces, and improve the stability of DNA duplex oligomers.[22]

Herein, we demonstrate that the well-defined xanthine-Na complexes on Au(111) can be only fabricated at elevated temperatures (Scheme 1): forming one-dimensional (1D) chain at ~430 K, and converting into a close-packed two-dimensional (2D) polymer at ~650 K. The 2D complex keeps adsorbed on Au(111) even at ~720 K, presenting as the most thermally stable organic polymer ever reported on Au(111).[23] Besides justifying the necessity of high-temperature, Na-rich environment for the prebiotic biosynthesis and the robustness of the polymer upon the harsh environment, this work further reveals an ability for the xanthine-Na complexes to induce significant electron transfer with the metal as inert as Au, lifting up Au atoms from the substrate by the strong interaction.

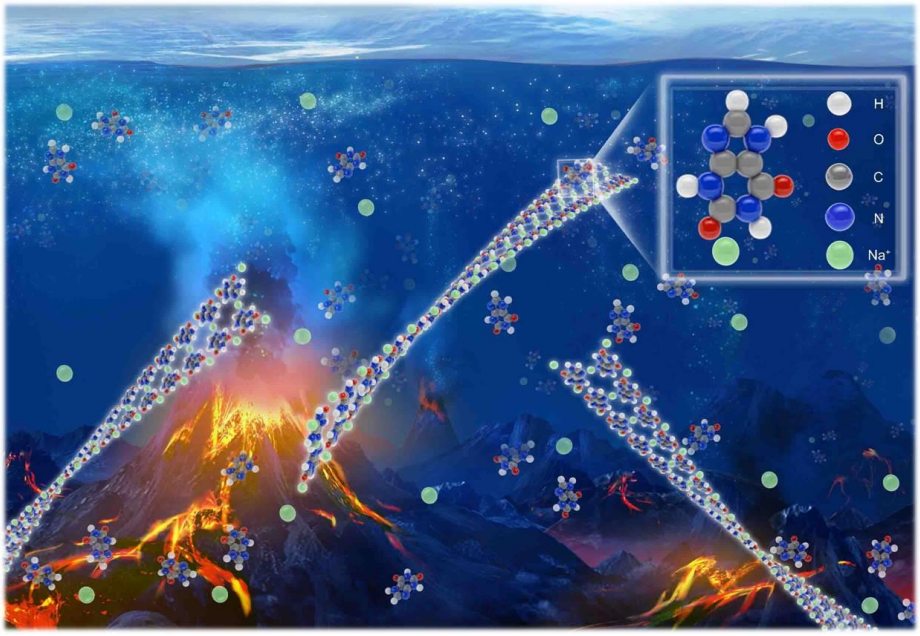

Scheme 1. Illustration of xanthine polymerization mimicking primordial submarine synthesis. Xanthine ($C_5H_4N_4O_2$, where carbon, nitrogen, oxygen, hydrogen atoms are in grey, blue, red and white, respectively) is one of the original exogenous nucleobases abundant on the prebiotic Earth. We demonstrate that xanthine can form the super-robust polymer with Na in a NaCl-rich and high-temperature environment.

To mimic the submarine adsorption–polymerization of xanthine, xanthine is deposited together with sodium chloride (NaCl) molecules onto an Au(111) surface. The on-surface reactions of organic molecules (*e.g.* purine molecules) with NaCl have been demonstrated previously.[24] Interestingly, well-defined xanthine-Na complexes only emerge after annealing at 430 K (for 20 min). This annealing temperature is very close to the temperature for the complete desorption of xanthine from Au(111), i.e. 433 K.[9] This means that co-deposition of NaCl resulted in a very stable xanthine structure that can survive temperatures at which normally xanthine if deposited alone would desorb. As shown in Figure 1A, the complex is presented in the form of individual 1D chains, oriented ⍰18° relative to the close-packed directions of the substrate. The chains cannot stretch over the step edges of the substrate, so their length is confined by the dimension of substrate terraces. On wide terraces, the chains can extend to 50 nm or longer (Figure S1). Close-view STM images reveal three distinct portraits of a single chain (Figures 2B–D). The image in Figure 1B represents the most common morphology, with parallel dimers (outlined by the dashed ellipse) piling up sideways, where each quasi-triangular motif in the dimer attributed to an individual xanthine molecule. In different tip states, additional circular protrusions (CPs, marked by the dashed circles) corresponding to Na atoms are visible in the middle of each xanthine dimer (Figure 1C) as well as on both sides of the chain, between two neighboring dimers (Figure 1D). Along the chain, the periodicity is 7.8 ± 0.2 Å; the chain width (depicted by the arrowed dashed line in Figure 1D) is 16.2 ± 0.3 Å.

To understand the 1D formation, we carried out DFT calculations, with two xanthine molecules and three Na atoms in each unit of the 1D complexes and three layers of Au substrate included (Figure 1E). The structural model after full relaxation shows the inner-chain periodicity of 7.67 Å, the chain width of 15.04 Å, and the chain orientation of 18.4° deviated from <1-10> directions of Au(111). Both the complex geometry and morphology based on this model are in good agreement with the experimental results (Figure 1F). The xanthine molecules are flatly adsorbed at a height of 3.29 Å above

the Au substrate. The Na atoms located in the middle of the dimer (Na_M) occupy top sites on Au(111) at a height of 2.63 Å, and interact with nitrogen (N) of xanthine by Na_M–N ionic bonding with a bond length of 2.58 Å; the Na atoms located on the chain sides (Na_S) sit on the three-fold hollow sites at a height of 2.48 Å and associate with the two neighboring oxygen (O) atoms of two xanthine molecules by Na_S–O ionic bonding with a bond length of 2.24 Å. The Na_M–N and Na_S–O bonding energies are of 0.47 eV and 0.58 eV.

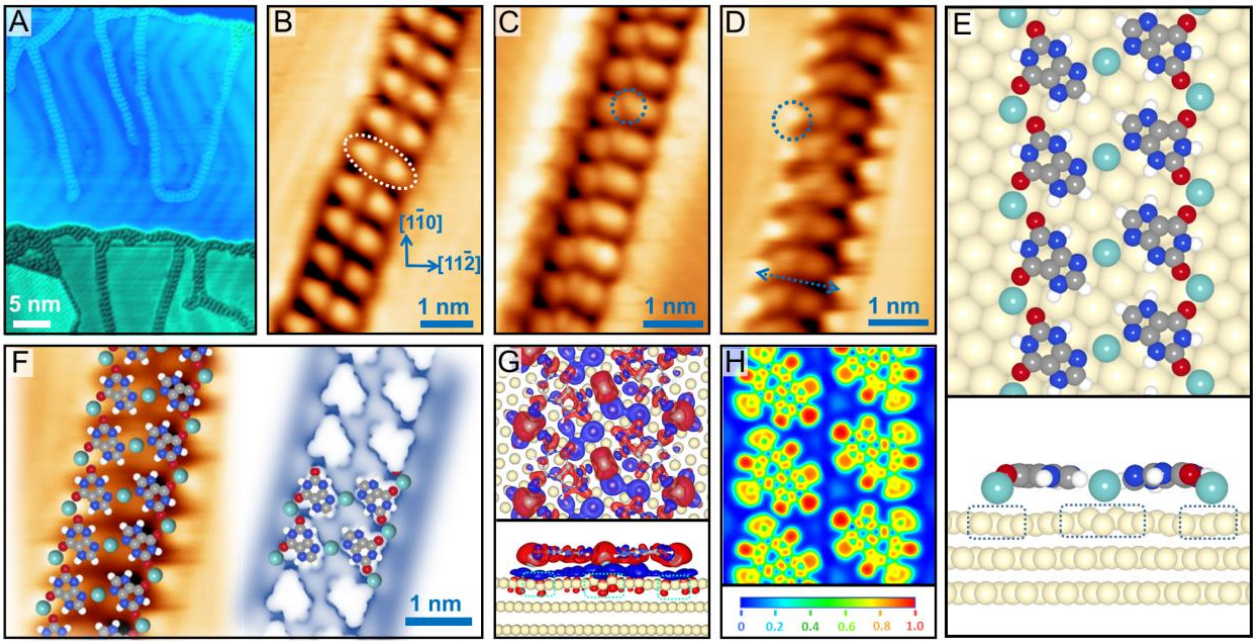

Figure 1. (A) STM image of the isolated chains formed at 430 K, a temperature very close to the desorption temperature of xanthine on Au(111). (B–D) Distinct morphology of a single chain obtained at different STM tip states, where each xanthine molecule is imaged as a quasi-triangular motif; the xanthine dimer is outlined by the dashed ellipse; the lobes corresponding to Na atoms are marked by the blue circles. (E) Top and side views of the structural model after full relaxation, containing the 1D complex and three layers of Au substrate; the local structural modification of the outmost Au layer induced by the complex is highlighted by the blue rectangles. (F) Comparison of the experimental and simulated images (with the structural model superimposed), showing a good agreement. (G) Top and side views of the electron density difference, and (H) ELF mapping of the 1D complex. In G, the red and blue colors indicate charge depletion and accumulation, and the isovalue is 0.01 e $Å^{-3}$.

Besides the evident electron donation to N and O of xanthine molecules, all Na in the complex have significant electron transfer with the Au substrate as well (Figure 1G). Based on the Bader charge analysis, each Na_M and Na_s donates 0.36 and 0.31 *e* to Au, respectively. Although the herringbone structure of Au(111) is visible after the xanthine-Na chain was fabricated (Figure 1A), pronounced corrugation corresponding to the local upward displacement of the Au atoms beneath the complex is revealed by the DFT modeling (outlined by the dashed rectangles in Figures 2E and 1G). As a result, the average adsorption energy of each Na is calculated to be 2.72 eV, and the total formation energy of each unit cell is 13.56 eV. The chains prefer being isolated from one another even at a relatively high coverage (Figure S1), largely due to the local positive charge of Na_s ions which provides repulsion between the chains. Consistently, the electron localization function (ELF) mapping of the 1D complexes (Figure 1H) shows the negative charge of O and N atoms of xanthine that interact with Na together with positive charge localized on both Na_S and Na_M.

This 1D structure remains unchanged until 470 K. At higher temperatures, structural transition starts. The chains transform into irregular islands at 476 K (the desorption temperature of NaCl, Figure S2). Further annealing to 650 K, a new ordered phase, *i.e.* 2D domains closely packed by parallel rows (denoted as '*CPR*'), is achieved (Figure 2A–C). According to the chemical structure analysis of xanthine made using infrared spectroscopy (Figure S3), no variation is induced when heating the molecules from RT to 650 K. Remarkably, the '*CPR*' polymerized domains maintain adsorbed on the surface even at a temperature as high as 720 K. No other structural phase is observed before full desorption. To further explore the stability, the 2D polymer was exposed to the air overnight. As shown in Figure S4, although the surface was contaminated seriously after exposure, well-defined, close-packed domains same to those of the pristine sample can be restored after annealing at 650 K. For the 2D polymer, the rows in different domains adopt three equivalent directions, at the angle of 20 ± 3 ° relative to <1-10> direction

of Au(111). The dimensions of the unit cell are $|\boldsymbol{a}|$= 7.9 ± 0.5 Å, $|\boldsymbol{b}|$ = 15.0 ± 0.5 Å, and the angle between the two vectors is 90 ± 2° (Figure 2B).

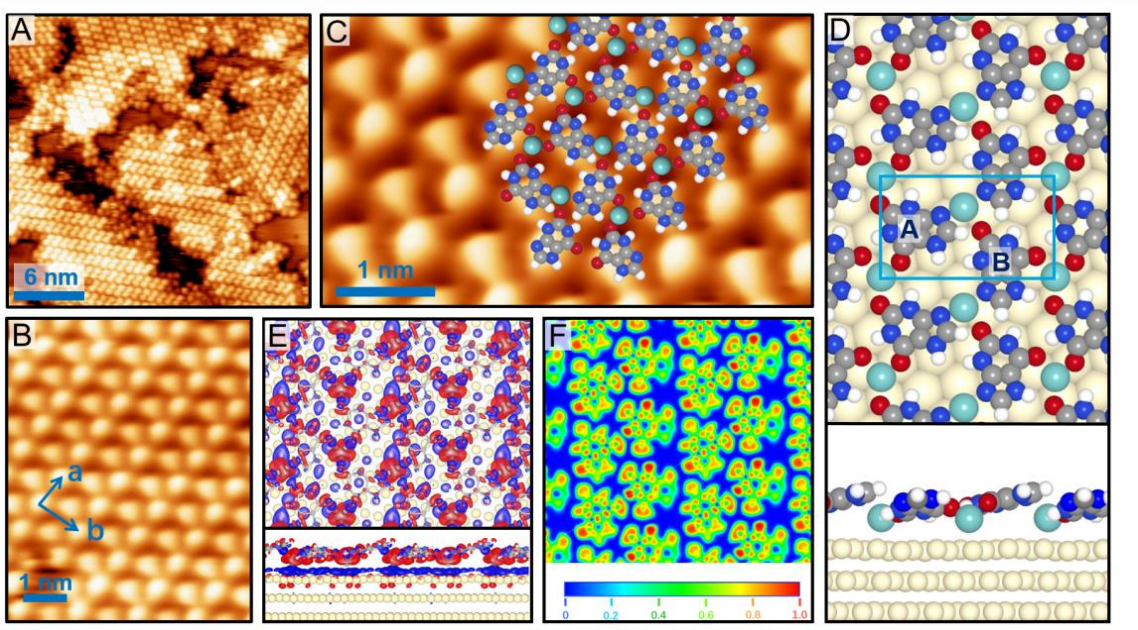

Figure 2. (A) Large scale, and (B–C) close-view STM images of the 2D domains of xanthine and Na obtained at 650 K, showing closely-packed parallel rows with the calculated structural model superimposed. (D) Top and side views of the structural model (unit cell is marked by the rectangle), (E) electron density difference (the isovalue 0.01 e $Å^{-3}$), and (F) ELF mapping for the 2D structure.

The optimized structural model of this 2D phase is presented in Figure 2D, where each unit contains two xanthine molecules and two Na atoms, with the three-layer Au slab included. Xanthine molecules in this case are not adsorbed in a flat geometry any more, but are slightly tilted on the surface, with molecules X_A and X_B indicated in Figure 2D making the angles of 11.8° and 12.5° relative to the surface. According to DFT calculations, all Na atoms occupy the face-centered cubic hollow sites of Au(111), with Na_O and Na_N being at a height of 2.51 Å and 2.56 Å, respectively. The lateral geometry, orientation, and morphology are well consistent with the experimental observation (Figure 2C). In each unit, one Na is coordinated with three O atoms of three neighboring xanthine molecules, resulting

in three Na–O ionic bonds (bond lengths of 2.27 Å, 2.34 Å, and 2.37 Å, respectively); the other Na is bonded with two N atoms and one O with Na–N and Na–O (bond lengths of 2.46 Å, 2.56 Å, and 2.29 Å, respectively). Similar to the 1D structure, there are strong xanthine–Na and Au–Na charge transfer in the electron density difference plot (Figure 2E) and significant charge localization in ELF mapping (Figure 2F). Na atoms in this case also induce evident corrugation of Au atoms with a charge transfer of 0.21 *e* to each Au. The average overall contribution of each Na to the 2D formation is –4.21 eV. The average adsorption energy of Na atoms is –2.90 eV per atom, more significant than that for the 1D complex.

The reaction between xanthine and NaCl is further explored by XPS. As shown in the high-resolution Na *1s* XP spectra (Figure 3A), a single peak centered at 1071.9 eV is observed from the sample of NaCl islands alone adsorbed on the Au(111) (Figure S5); the peak is shifted towards a lower binding energy for the xanthine-Na complex after reacted with xanthine. For 1D complex, the Na *1s* peak contains three distinct components: in addition to the signal of Na−Cl bonding at 1071.9 eV,[25] there are two subpeaks at 1071.4 and 1070.8 eV attributed to Na–O and Na–N bonding from the oxygen/nitrogen-containing moieties coupling with the Na,[24,26] respectively; the area ratio of the latter two peaks is approximately 2:1, matching the calculated model based on the STM results in which there are four Na–O and two Na–N bonds per unit cell (Figure 1E). For 2D complex, whilst the area ratio of the subpeaks corresponding to Na–O and Na–N bonding is same to that of 1D case (which again is consistent with the number of Na-O and Na-N bonds per cell remaining the same, Figure 2D), the third peak corresponding to Na−Cl bonding vanishes, as NaCl has been completely desorbed from the surface at 476 K. The position of both peaks for the 2D phase is found to slightly shift towards higher binding energies, consistent with the varied charge donation and binding environment for Na: each Na atom forms three ionic bonds with three neighboring O/N atoms of xanthine in the 2D phase,

while forms only two bonds with two N/O atoms in the 1D chain. Consistently, the Cl *2p* signal is completely vanished for the 2D phase (Figure 3B), due to desorption of Cl upon high temperature annealing;[27] meanwhile, both peaks (199.0 and 200.6 eV) for 1D complex shrink and shift by 0.1 eV to lower binding energies compared with those in NaCl, implying the dissociation of Cl ions with Na and coordination with the metal substrate, consistent with the reported reaction of teraphthalic acid with NaCl on Cu(100).[24]

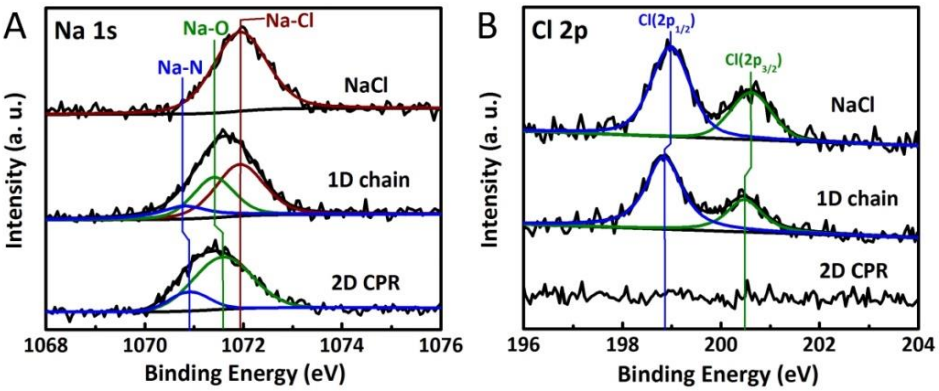

Figure 3. (A) Na *1s* spectra, where the 1D/2D complexes' peak blue-shifts relative to that of NaCl. (B) Cl *2p* spectra, where the peaks shift relative to those of NaCl for the 1D complex, and completely vanish for the 2D xanthine-Na.

The super-robustness of xanthine-Na complexes superior to the reported biomolecules[26–28] and metal-organic complexes[29–30] on Au(111) is thus attributed to the following synergistic advantages: (i) compared with many other organic molecules [*e.g.* terephthalic acid [24]] which are easily decomposed at a relatively low temperature (~453 K), xanthine itself has a high thermochemical stability, showing no degeneration after long annealing at high temperatures; (ii) O and N atoms in xanthine enable multiple binding sites for the interaction with Na; (iii) Na atoms not only provide strong ionic bonding with xanthine to form the extended and robust polymers, but also pin the polymers firmly to the substrate by Na-Au metallic bonding. The high desorption temperature of the 2D xanthine-Na complex (720 K) is also associated with its close-packed organization. As a comparison, when hypoxanthine

($C_5H_4N_4O$, a purine molecule that can be oxidized to be xanthine and uric acid via xanthine-oxidase catalysis) interacts with NaCl, stable complexes are also obtained on Au(111). However, even for the most thermostable phase of hypoxanthine-Na complexes on Au(111) (showing as open honeycomb networks), the desorption temperature is less than 520 K, which is much higher than that of pure hypoxanthine but lower than that of xanthine-Na polymer. Considering the similarity between hypoxanthine and xanthine and the strong ionic bonding between the N and O atoms of hypoxanthine with Na, the lower desorption temperature is very likely attributed to its less dense lateral arrangement. The results suggest that the lateral arrangement of the purine-Na complexes also plays an important role for its high robustness on the suface.

In summary, by mimicking the prebiotic submarine synthesis with a simplified model, *i.e.* reaction of xanthine and NaCl on Au(111), we justifiy the necessity of submarine high temperature condition: (i) richness of Na allows the instant and sufficient ionic binding with xanthine; (ii) the robust xanthine-Na polymers can be only formed at a high temperature. The obtained xanthine-Na complexes are the most robust organic polymer ever reported on Au(111). Moreover, Na in the 1D/2D xanthine-Na complexes show evident charge transfer with Au: each Na donates up to ~0.3 *e* to an Au atom and can lift the Au atoms up. At the molecular level, the basis of life is in various redox reactions, which provide energy for growth, metabolism and all other physiological processes. The strong electron donation of such complexes could possibly play a role in the initial redox reactions for the prebiotic biochemical synthesis.

ACKNOWLEDGMENTS

This work is financially supported by the National Natural Science Foundation of China (21473045, 51772066, 52073074, 22002103), and State Key Laboratory of Urban Water Resource and Environment, Harbin Institute of Technology (2021TS08).

Conflict of interest

The authors declare no conflict of interest.

Keywords: purine oligomer • organometallic complexes • prebiotic synthesis • origin of life • scanning tunneling microscopy

REFERENCES

[1] N. Ichihashi, T. Yomo, *Life* **2016**, *6*, 26.

[2] N. Lavado, J. G. Concepción, M. Gallego, R. Babiano, P. Cintas, *Org. Biomol. Chem.* **2019**, *17*, 5826–5838.

[3] Shapiro, *Origins Life Evol. B.* **1995**, *25*, 83–98.

[4] A. L. Reysenbach, E. Shock, *Science* **2002**, *296*, 1077–1082.

[5] N. Kitadai, R. Nakamura, M. Yamamoto, K. Takai, N. Yoshida, Y. Oono, *Sci. Adv.* **2019**, *5*, 7848–7856.

[6] W. H. Yu, N. Li, D. S. Tong, C. H. Zhou, C. X. Lin, C. Y. Xu, *Appl. Clay Sci.* **2013**, *80–81*, 443–452.

[7] J. P. Ferris, *Origins Life Evol. B.* **2002**, *32*, 311–332.

[8] J. P. Ferris, *Phil. Trans. R. Soc. B* **2006**, *361*, 1777–1786.

[9] C. Chen, H. Q. Sang, P. C. Ding, Y. Sun, M. Mura, Y. Hu, L. Kantorovich, F. Besenbacher, M. Yu, *J. Am. Chem. Soc.* **2018**, *140*, 54–57.

[10] M. Wu, R. Kempaiah, P. J. Huang, V. Maheshwari, J. W. Liu, *Langmuir* **2011**, *27*, 2731–2738.

[11] R. Otero, M. W. Xu, R. E. Lukas, A. Kelly, E. Lægsgaard, I. Stensgaard, J. Kjems, L. N. Kantorovich, F. Besenbacher, *Angew. Chem. Int. Ed.* **2008**, *47*, 9673–9676.

[12] A. Ciesielski, M. E. Garah, S. Masiero, P. Samorì, *Small* **2016**, *12*, 83–95.

[13] M. Östblom, B. Liedberg, L. M. Demers, C. A. Mirkin, *J. Phys. Chem. B* **2005**, *109*, 15150–15160.

[14] R. A.Harkness, *J. Chromatogr. B* **1988**, *429*, 255–278.

[15] Z. K. Shihabi, M. E. Hinsdale, A. J. Bleyer, *J. Chromatogr. B* **1995**, *669*, 163–169.

[16] C. Scazzocchio, H. N. Arst, *Nature* **1978**, *274*, 177–179.

[17] Z. Martins, O. Botta, M. L. Fogel, M. A. Sephton, D. P. Glavin, J. S. Watson, J. P. Dworkin, A. W. Schwartz, P. Ehrenfreund, *Earth Planet. Sci. Lett.* **2008**, *270*, 130–136.

[18] S. J. Sowerby, G. B. Petersen, *Origins Life Evol. Biospheres* **1999**, *29*, 597–614.

[19] G. Wachtershauser, *Proc. Natl. Acad. Sci. U.S.A* **1988**, *85*, 1134–1135.

[20] A. Fardous, S. Gondal, Z. Shah, K. Ahmad, *Pak. J. Bot.* **2010**, *42*, 2411–2421.

[21] L. P. Knauth, *Nature* **1998**, *395*, 554–555.

[22] R. Owczarzy, *Biochemistry* **2004**, *43*, 3537–3554.

[23] Y. F. Geng, P. Li, J. Z. Li, X. M. Zhang, Q. D. Zeng, C. Wang, *Coordin. Chem. Rev.* **2017**, *337*, 145–177.

[24] D. Skomski, S. Abb, S. L. Tait, *J. Am. Chem. Soc.* **2012**, *134*, 14165–14171.

[25] J. Q. Lu, M. F. Luo, C. Li, *React. Kinet. Catal. Lett.* **2005**, *86*, 219–224.

[26] J. Sharma, T. Gora, J. D. Rimstidt, R. Staley, *Chem. Phys. Lett.* **1972**, *15*, 232–235.

[27] G. N. Kastanas, B. E. Koel, *Appl. Surf. Sci.* **1993**, *64*, 235–249.

[28] S. Abb, L. Harnau, R. Gutzler, S. Rauschenbach, K. Kern, *Nat. Commun.* **2016**, *7*, 10335–10341.

[29] Y. Li, J. Xiao, T. E. Shubina, M. Chen, Z. L. Shi, M. Schmid, H. P. Steinruck, J. M. Gottfried, N. Lin, *J. Am. Chem. Soc.* **2012**, *134*, 6401–6408.

[30] C. Chen, P. C. Ding, M. Mura, Y. H. Chen, Y. Sun, L. N. Kantorovich, H. Gersen, F. Besenbacher, M. Yu, *Angew. Chem. Int. Ed.* **2018**, *57*, 16015–16019.